Effect of environmental forcing on the biomass, production and growth rate of size-fractionated phytoplankton in the central Atlantic Ocean

María Huete-Ortega [a,*], Alejandra Calvo-Díaz [b,c,1], Rocío Graña [d],
Beatriz Mouriño-Carballido [a], Emilio Marañón [a]

[a] Departamento de Ecología y Biología Animal, Universidad de Vigo, Campus Lagoas-Marcosende 36310 Vigo, Spain
[b] Instituto Español de Oceanografía, Centro Oceanográfico de Xixón, 33212 Xixón, Spain
[c] Department of Marine Biology, University of Vienna, 1090 Vienna, Austria
[d] Grupo de Oceanografía Física, Universidad de Vigo, Campus Lagoas-Marcosende 36310 Vigo, Spain

ARTICLE INFO

ABSTRACT

To ascertain the response of phytoplankton size classes to changes in environmental forcing, we determined size-fractionated biomass, carbon fixation and growth (production/biomass) rates in surface waters along the central Atlantic Ocean (26°N–5°S). As a result of the enhanced input of nutrients into the euphotic layer and the higher water column stability found at the equatorial upwelling, we observed increases not only in phytoplankton biomass and primary production, but also in turnover rates, suggesting nutrient limitation of phytoplankton physiology in the oligotrophic central Atlantic. The phytoplankton groups analysed (pico-, small nano-, large nano- and micro-phytoplankton) showed different responses to the equatorial environmental forcing, in terms of carbon biomass, primary production and growth rate. Large nano- and micro-phytoplankton consistently showed higher growth rates and carbon fixation to chl a ratios than smaller phytoplankton. We observed a higher stimulating effect of increased nitrate supply on the small phytoplankton growth rates. This observation can be explained by the dynamics of the equatorial upwelling, where the continuous but small nutrient input into the euphotic layer provide a competitive advantage for smaller cells adapted to oligotrophic conditions. The size-fractionated approach shown here reveals important group-specific differences in the response to environmental forcing, which cannot be appreciated in bulk measurements of the whole community.

© 2011 Elsevier B.V. All rights reserved.

1. Introduction

Phytoplankton size structure is a critical property of pelagic ecosystems as it largely determines their food-web organisation and, consequently, their biogeochemical functioning (Kiørboe, 1993; Legendre and Rassoulzadegan, 1996; Marañón, 2009). Communities dominated by small cells (<5 μm in Equivalent Espherical Diameter, ESD), typical of oligotrophic waters, are characterised by the recycling of matter within the microbial food web and, in consequence, by a small downward carbon export (Azam et al., 1983; Goldman, 1988). By contrast, the dominance by larger cells (>5 μm in ESD), commonly observed in turbulent and nutrient-rich areas, favours the transfer of organic matter through short-food chains towards higher trophic levels as well as its sedimentation towards the deep ocean, thus increasing the potential of these ecosystems for CO_2 sequestration (Chisholm, 1992; Cushing, 1989). In addition, both chemical and physical characteristics of ecosystems are key factors in controlling the size distribution of phytoplankton community. Among other factors, a higher nutrient supply tends to stimulate in particular the growth of large phytoplankton and the upwelling water motion increases the time of permanence of large cells inside the photic layer, thus increasing primary production (Kiørboe, 1993; Malone et al., 1993; Parsons and Takahashi, 1973).

It is commonly accepted that in pelagic ecosystems picophytoplankton constitute a background component of the phytoplankton community whose biomass and primary production keep relatively constant independently of changes in the environment, and that most of the geographical and temporal variability observed in these variables is due to the response of large phytoplankton to environmental forcing (Raimbault et al., 1988; Rodríguez et al., 1998; Thingstad and Sakshaug, 1990). However, recent studies have demonstrated that, in addition to the spatial and temporal variability observed for picophytoplankton abundance in both open ocean and coastal ecosystems (Calvo-Díaz and Morán, 2006; Li et al., 2006; Partensky et al., 1996; Zubkov et al., 1998), there is also a response of

smaller cells, in terms of both biomass and production, to the enrichment of oligotrophic regions of the ocean, although the magnitude of this response may be lower than that registered for larger phytoplankton (Barber and Hiscock, 2006; Glover et al., 2007; Tarran et al., 2006). Given the importance of the nutrient-impoverished regions of the ocean in global biogeochemical cycles (Longhurst, 1995), it is essential to improve our current knowledge about which factors determine the phytoplankton distribution and activity in pelagic ecosystems and over which size fractions of phytoplankton they are acting.

Numerous studies have focused on the simultaneous analysis of size-fractionated biomass and productivity of phytoplankton in the ocean. Most of them have been conducted in particular geographic areas (Cermeño et al., 2005a; Han and Furuya, 2000; Jochem and Zeitzschel, 1989; Tamigneaux et al., 1999), and in those works carried out in the open ocean over large spatial scales, biomass has been almost always estimated from chlorophyll *a* concentrations, rather than from estimations of cell carbon content (Marañón et al., 2001; Poulton et al., 2006). Moreover, instead of covering all size classes [the pico- (0.2–2 μm in ESD), nano- (2–20 μm in ESD) and micro-phytoplankton (>20 μm in ESD) (Sieburth, 1979)], studies generally have focused on the picophytoplanktonic component of the community (Li and Harrison, 2001; Worden et al., 2004; Zubkov et al., 1998) or they have only distinguished between picophytoplankton and large phytoplankton (including within this group all cells >2 μm ESD) (*i.e.* Jochem and Zeitzschel, 1989; Joint and Pomroy, 1986; Poulton et al., 2006). However, recent studies have highlighted the importance of conducting this kind of analysis for the whole phytoplankton size range, in order to better understand the carbon fluxes through the microbial plankton community (*e.g.* Latasa et al., 2005). This importance arises from the different dynamics, in both biomass and production, showed by the main phytoplankton taxonomic groups under different environmental conditions, which can be translated into the different contribution of each group to the carbon cycling.

In addition, a more informative approach to the study of the functioning of planktonic communities is the analysis of the variability of phytoplankton growth rates in combination with primary production estimations and carbon biomass measurements for the different phytoplankton size groups. In this sense, the simultaneous variation of primary production and growth rates under changing environmental forcing will mean that phytoplankton are not only limited in their standing stocks but also in their physiological state (Goldman et al., 1979). However, the studies carried out in order to determine the growth rates for different size groups of phytoplankton in the field are very scarce, and most of them have considered only the smaller size classes such as the picophytoplankton (*i.e.* Hirose et al., 2008; Liu et al., 1997; Zubkov and Tarran, 2008).

The latitudinal variability in nutrient concentration and water column structure of the tropical and subtropical Atlantic Ocean is well documented (*e.g.* Marañón et al., 2000, 2001; Poulton et al., 2006). A "Typical Tropical Structure" (TTS; Herbland and Voituriez, 1979), whereby a nutrient-depleted upper mixed layer is separated from a light-limited deep layer by a strong density gradient, is found in those regions under the influence of the oligotrophic gyres, while a persistent upwelling takes place in the equatorial region (Longhurst, 1993; Monger et al., 1997; Pérez et al., 2005a). This equatorial upwelling is the result of the differential effect of the Ekman transport on both sides of the Equator, which causes the entrance into the photic layer of nutrient-rich water from the equatorial undercurrent and the shallowing of the deep chlorophyll *a* maximum (DCM) that typically develops at or close to the pycnocline depth (Longhurst, 1993; Tomczak and Godfrey, 1994). The study of the variability of biotic and abiotic factors throughout a long latitudinal transect of the Atlantic central ocean crossing the equatorial upwelling constitutes a good opportunity for testing the effect of environmental forcing, mainly nutrient availability and water-column structure, on the

dynamics of the phytoplankton community. Here we report the latitudinal variability of size-fractionated phytoplankton carbon biomass, primary production and growth rates in a survey conducted from 26°N to 5°S along the ~29°W meridian, with two main objectives: 1) to determine the response of the different size groups of phytoplankton, in terms of both biomass and production, to changes in water column stability and nutrient availability; and 2) to determine the latitudinal variability of size-fractionated phytoplankton growth rates in order to assess the physiological response of different size classes to environmental forcing and in particular nutrient supply. The results and conclusions shown in the present study are complementary to those reported for the same oceanographic survey by Moreno-Ostos et al. (2011), who analyse the differential impact of light on small and large phytoplankton standing stocks and production.

2. Methods

2.1. Sampling, hydrography, irradiance and nutrients

We sampled 10 stations during the TRYNITROP (*Trichodesmium* and N_2 fixation in the tropical Atlantic) cruise, carried out in November–December 2007 in the tropical Atlantic Ocean (Fig. 1) on board R/V *Hespérides*. At each sampling station, vertical profiles (0–300 m) of temperature, salinity and *in situ* fluorescence were obtained using a Conductivity–Temperature–Depth (CTDSBE911)
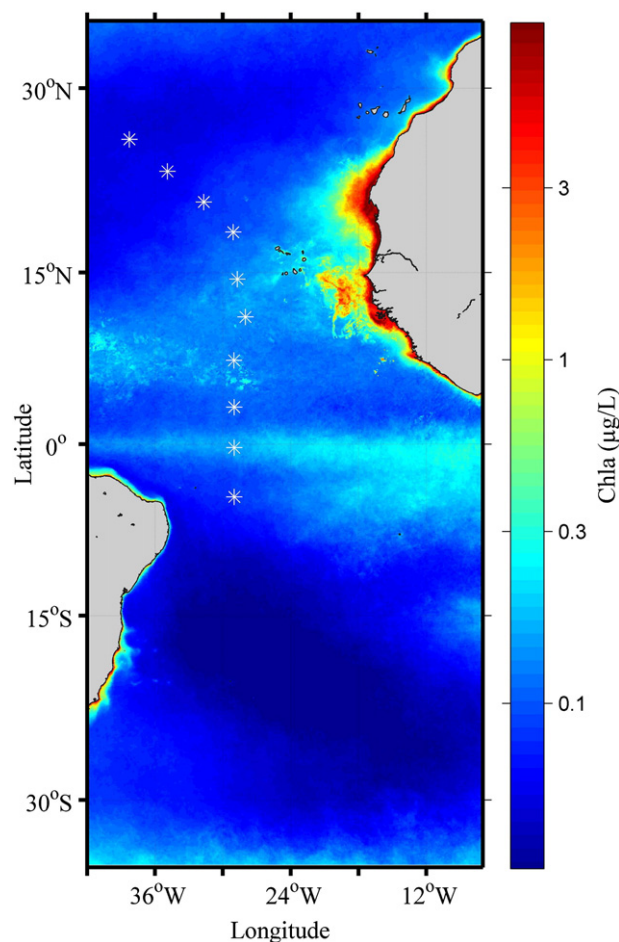

Fig. 1. Location of the sampling stations superimposed on a map of the climatological mean surface chlorophyll *a* concentration for the period September–November of the years 2002–2008 in the Atlantic Ocean. Ocean colour data are from MODIS Aqua (9 km).

probe attached to a rosette sampler equipped with Niskin bottles. Using the density computed from the temperature and salinity data distributed in 1 m intervals, we calculated the Brunt-Väisälä frequency (BV), averaged over the upper 125 m, as a proxy of water column stability (Bray and Fofonoff, 1981). Sampling was conducted before dawn and different water subsamples were collected from the Niskin bottles to determine nutrient concentration, phytoplankton biomass and abundance, chlorophyll *a* concentration and primary production.

During our cruise and a subsequent cruise conducted along the same track, in April–May 2008, 16 vertical profiles of photosynthetically active irradiance (PAR) were obtained at noon with a Satlantic OCP-100FF radiometer. A highly significant relationship was obtained between the depth of the 1% PAR (Z_{eu}) and the depth of the DCM identified by *in situ* fluorescence (Z_{DCM}): $Z_{eu} = 9.3 + 0.98 \times Z_{DCM}$ ($r^2 = 0.93$, p<0.001, $n = 16$). This relationship was used to calculate Z_{eu} and the light extinction coefficient (K_d) in all sampled stations.

Nanomolar and micromolar nutrient concentrations were determined with a segmented-flow automatic analyser (Technichon/Bran Luebbe), following the method of Raimbault et al. (1990). The concentration of nitrate, phosphate and silicate were highly correlated along the latitudinal transect ($r = 0.97$, p<0.001, $n = 109$ and $r = 0.85$, p<0.001, $n = 103$ for nitrate *vs.* phosphate and nitrate *vs.* silicate, respectively). In addition, neither silicate (mean concentration in the upper mixed layer was 1.5 ± 0.9 [$\pm$sd] μmol L^{-1}) nor phosphate (the mean nitrate to phosphate ratio in the upper mixed layer was 3.0 ± 1.6 [$\pm$sd]) were likely to be limiting. Therefore, our analysis was subsequently focused exclusively on the latitudinal variability of nitrate and its limiting role on the phytoplankton metabolism. The nitracline depth was defined as the depth below which nitrate concentration was equal to 0.5 μmol L^{-1}. Vertical nitrate fluxes into the euphotic layer were calculated from the product of the estimated diffusion coefficients (kz) and the gradients of nanomolar nitrate concentration, computed across the depth of the euphotic layer by using linear interpolation. The photic layer depth corresponded to the 1% of PAR (photosynthetic active radiation). Vertical diffusivity (kz) was estimated from Osborn (1980) as:

$$kz = e\left(\varepsilon / N^2\right)$$

where e is a mixing efficiency (e = 0.2 herein), ε is the dissipation rate of turbulent kinetic energy, and N is the Brunt-Väisälä frequency averaged over depth intervals of 10 m length. Assuming that the dissipation of turbulent kinetic energy balances the local production due to the shear induced by the wind stress, ε was parameterized from wind data (Terray et al., 1996) as:

$$\varepsilon = u^{*3} / kz$$

where k is the von Karman's constant (0.4) and u* is the friction velocity, related to the surface wind stress by

$$\tau = \rho_w u^{*2} = \rho_a C_D W^2$$

where ρ_w is the water density, ρ_a is the air density, C_D is a drag coefficient and W is the wind speed determined with an Aanderaa meteorological station during the cruise. For each station, wind speed was averaged during 24 h before the CTD sampling. The drag coefficient was 1.14×10^{-3} for $4 < W \leq 10$ m s^{-1} and computed as $C_D = (0.49 + 0.065\,W) \times 10^{-3}$ for $10 < W < 26$ m s^{-1} (Large and Pond, 1981).

2.2. Size-fractionated chlorophyll a concentration

Two replicates of 500 mL surface seawater were sequentially filtered through 40 μm net filters and 20, 10, 5, 3, 2, 0.8 and 0.2 μm polycarbonate filters under low vacuum pressure (<50 mm Hg). In

order to avoid the undersampling of larger cells, for 40, 20, 10 and 5 μm filters, the whole 500 mL were filtered, whereas for 3, 2, 0.8 and 0.2 μm filters only 250 mL were filtered. After filtration, pigments were extracted in 90% acetone during 24 h in the dark and at 4 °C. Chlorophyll *a* (chl *a*) concentration was estimated with the non-acidification technique using a Turner Designs Fluorometer (TD-700), previously calibrated with pure chl *a*. The detailed analysis of each of the 8 assayed size classes was used to calculate the size scaling of carbon fixation and abundance, which will be reported elsewhere. In the present study, to calculate the chl *a* concentration in the phytoplankton size classes commonly used in the literature, concentrations measured in different filters were added: 0.2 and 0.8 μm for picophytoplankton (<2 μm in ESD), 2 and 3 μm for small nanophytoplankton (2–5 μm in ESD), 5 and 10 μm for large nanophytoplankton (5–20 μm in ESD), and 20 and 40 μm for microphytoplankton (>20 μm in ESD). Total chl *a* values were calculated as the sum of all size-fractionated chl *a* concentrations.

2.3. Size-fractionated carbon fixation rate

Photosynthetic carbon fixation rates were measured with the ^{14}C uptake kinetic. One-litre polycarbonate bottles (3 transparent and 1 dark bottles) were filled with surface seawater from each station, taking care to avoid any light shock to the plankton populations. To always sample at the 80% of surface irradiance, sampling depths were selected by applying the calculated K_d for each station to the Lambert–Beer equation. Bottles were inoculated with ~100 μCi NaH^{14}CO$_3$ and then incubated during 5–7 h in on-deck flow-through incubators which were cooled with running surface seawater. All incubations were started at dawn and were finished about 1–2 h after noon. The irradiance received by the incubation bottles was attenuated to 80% using a neutral density screen. At the end of the incubation time, water samples were sequentially filtered, under low vacuum pressure, through the same types of filters used for the estimation of the size-fractionated chl *a* concentration. In order to ensure adequate sampling of larger cells, for 40, 20, 10 and 5 μm filters, the whole content of the 1-L bottles was filtered, whereas in the case of the 3, 2, 0.8 and 0.2 μm filters only 500 mL were filtered. The unassimilated dissolved inorganic ^{14}C was removed from the filters by exposing them to concentrated HCl fumes during 10–12 h. Filters were then placed in 5-mL scintillation vials to which 4 mL of scintillation cocktail were added. The radioactivity of each filter was measured with a Wallac scintillation counter. Disintegrations per minute (DPMs) from dark bottle filter were subtracted from the DPMs of each light bottle filter and the carbon fixation rate of each size class was calculated taking into account the filtered volume and assuming a constant ambient DIC concentration of 25,956 mg m^{-3}. To obtain daily carbon fixation rates, the hourly rates were multiplied by the duration of the daylight period and it was assumed that 20% of the carbon fixed during the light period is lost through respiration during the night (Geider, 1992). Carbon fixation rates of each light bottle for pico-, small nano-, large nano- and micro-phytoplankton were calculated from the rates determined for each individual size class, as explained before for chl *a* concentration, and were subsequently averaged. Total carbon fixation rates for each sample were calculated as the sum of the size-fractionated carbon fixation rates.

2.4. Phytoplankton cell size and abundance

The abundance of surface pico- (<2 μm in ESD) and small nanophytoplankton (2–5 μm in ESD) was determined by flow cytometry using a FACSCalibur flow cytometer (Becton Dickinson) with a laser emitting at 488 nm. Samples (4 mL) were fixed with 1% (v/v) paraformaldehyde and 0.05% glutaraldehyde, frozen in liquid nitrogen and subsequently kept at −80 °C until analysis at the laboratory. Aliquots of each sample were used for the analysis of the cell size and abundance of picophytoplankton and small nanophytoplankton. As our aim was to

determine the total cell abundance in a given size range, taxonomical groups such as *Prochlorococcus sp.* or *Synechococcus sp.* were not distinguished. Calibration of the cytometer flow rate was performed daily (Marie et al., 1999) for estimating the abundance of both size ranges. In order to increase the number of counting events, the analyses for large picoeukaryotes and small nanophytoplankton were always conducted during 10 min at high flow rate (around 40 μL min^{-1}). An empirical calibration between relative side scatter (SSCrel) and cell diameter (D) following Zubkov et al. (1998) was used to estimate the individual cell biovolume (V) of picophytoplankton cells, $D = 1.0049 \times$ SSCrel $+ 0.6297$. For the small nanophytoplankton, V was estimated using a calibration curve that relates the light scattering signal (FSC) to cell biovolume estimated by image analysis, $\log V = 0.0079 \times FSC + 1.0699$ (Rodríguez et al., 1998). This latter calibration curve was constructed with measurements of monospecific cultures of *Nannochloropsis gaditana* (2–5 μm), *Isochrysis galbana* (3–5 μm), *Phaeodactylum tricornutum* (3–6 μm), *Rhodomonas* sp. (7 μm), *Heterocapsa* sp. (15 μm) and *Alexandrium* sp. (20 μm).

Large nano- (5–20 μm in ESD) and micro- (>20 μm in ESD) phytoplankton were determined by image analysis under an inverted microscope. With the aim of increasing the number of large-sized cells sampled, we used 2 replicates of 2 L of surface seawater. Samples were filtered through 5 μm polycarbonate filters and then the material collected on the filters was gently resuspended with 0.2 μm-filtered seawater until completing a sample volume of 125 mL. One of these replicate samples was fixed with 2% Lugol's solution whereas the other one was fixed with 4% formaldehyde. Samples were stored in the dark until their analysis following the method of Utermöhl (Lund et al., 1958). Subsamples of 100 mL in volume were allowed to settle in sedimentation columns for 48 h and then counted using an Olympus IX50 inverted microscope. A magnification of 100× was used for large forms, 200× for intermediate forms and 400× for smaller forms. In the samples fixed with Lugol's solution, the cell biovolume of ~400 cells was determined using the geometric shapes recommended in Olenina et al. (2006) and the NIS-Elements BR 3.0 image analysis programme. Samples fixed with formaldehyde's solution were only analysed in order to estimate the cell abundance and biovolume of coccolithophores. In the case of chain-forming species (*i.e. Trichodesmium* spp., *Rhizosolenia* spp. or *Pseudonitzchia* spp.), measurements of the average cell size of the cells that formed each trichome or chain and the size of each trichome and chain were carried out in order to estimate the cell abundance of these species in each sample.

2.5. Phytoplankton carbon biomass and growth rates

Picophytoplankton biovolume (V) was converted to carbon biomass (C) using the conversion factor of 235 fg C μm^{-3} obtained from averaging the values proposed in Worden et al. (2004) for the different picophytoplankton groups. Small nanophytoplankton carbon was estimated with the conversion equation proposed by Verity et al. (1992), pg C cell$^{-1} = 0.433 \times V^{0.863}$, and large nano- and microphytoplankton carbon was calculated according to Montagnes and Berges (1994), pg C cell$^{-1} = 0.109 \times V^{0.991}$. Phytoplankton carbon biomass (Phyto-C) was estimated by multiplying cell abundance by cellular carbon biomass and the resulting values were added in order to obtain the Phyto-C for pico-, small nano-, large nano- and microphytoplankton. Growth (turnover) rates for both total and size-fractionated phytoplankton were calculated by dividing production (carbon fixation rates) by biomass, as advised by Kirchman (2002).

3. Results

3.1. Hydrography and chlorophyll a concentration

The vertical distribution of temperature shown in Fig. 2a indicates strong thermal stratification in the upper mixed layer (UML) through-
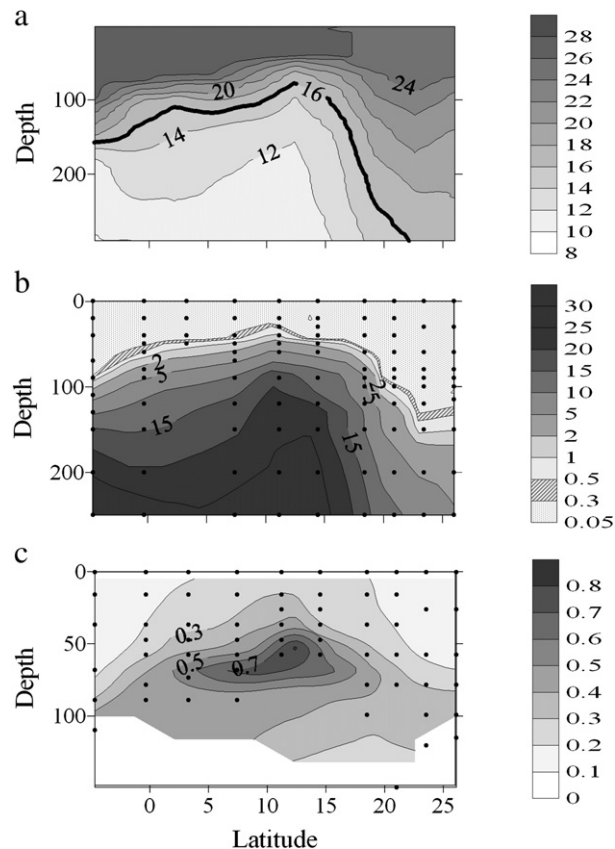

Fig. 2. Latitudinal and vertical variability of a) temperature (°C), b) nitrate concentration (μmol L^{-1}) and c) chlorophyll *a* concentration (mg m^{-3}). Positive and negative latitude values correspond to the North and South hemisphere, respectively.

out the transect. Warmer UML temperatures (~28 °C) occurred south of 17°N, coinciding with the strongest stratification of the water column. The 16 °C isotherm was relatively shallow (<120 m) between 17°N and the Equator, indicating the upwelling of cold and nutrient-rich deep waters in this region. Thus, the equatorial upwelling was detected slightly displaced northwards from the Equator, as it is typical for the sampling season (Pérez et al., 2005a, 2005b). Accordingly, the influence of the environmental forcing associated to this hydrodynamic feature was considered to be between 17°N and the Equator. Very low nitrate concentrations (<0.5 μM) were measured in the UML along the whole transect and those stations most affected by upwelling presented higher sub-surface concentrations (Fig. 2b). Similarly, the highest chlorophyll *a* concentration (chl *a*) values (>0.25 mg m^{-3}) in the UML were found in those stations most influenced by the equatorial upwelling, whereas near both ends of the transect UML chl *a* below 0.2 mg m^{-3} was measured, coinciding with the beginning of the subtropical gyres (Fig. 2c). A deep chl *a* maximum (DCM) was observed throughout the transect at the base of the photic layer. As a consequence of the equatorial upwelling, the DCM was shallower (~60 m) between 15°N and the Equator.

Coherent patterns in the latitudinal variability of water column stability (indicated by the Brunt-Väisälä frequency averaged over the upper 125 m), PAR extinction coefficient (K$_d$), nitracline depth and nitrate diffusive fluxes computed across the euphotic zone were observed during the transect, reflecting the environmental forcing associated with the equatorial upwelling (Fig. 3a and b). In general, stronger water stability was observed between 15°N and the Equator, as a result of the upwelling of cold subsurface waters. In the case of K$_d$, higher values (>0.05 m^{-1}) were found between ca. 15°N and the Equator, reflecting the presence of higher phytoplankton abundances in this region. Northwards and southwards of these latitudes,
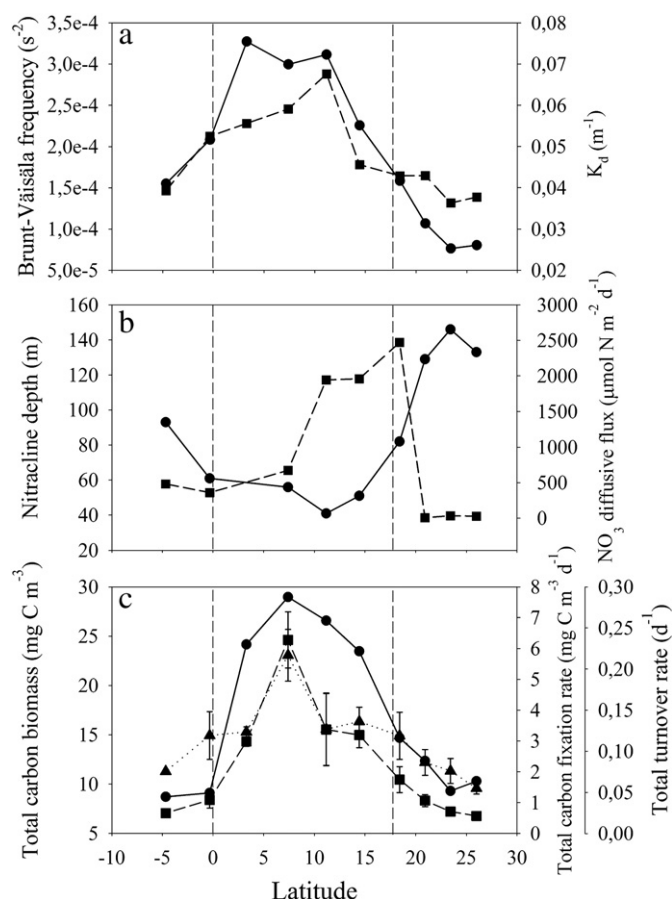
Fig. 3. Latitudinal variability of a) the Brunt-Väisälä frequency (circles, solid lines) and K_d (squares, dashed lines), b) the nitracline depth (circles, solid lines) and nitrate diffusive flux computed across the euphotic zone (squares, dashed lines), and c) surface total carbon biomass (circles, solid lines), total carbon fixation rates (squares, dashed lines), and total turnover rate (triangles, dotted lines). Error bars indicate 1 SD. Vertical dashed lines point out those stations under the influence of the Equatorial upwelling. Latitude values as in Fig. 2.

progressively smaller K_d values were measured, indicating the presence of very clear and oligotrophic waters with low phytoplankton abundances. Nitracline depth and nitrate diffusive flux showed opposite latitudinal patterns, as it is supported by the significant, inverse correlation found between both variables ($r = -0.67$, $p < 0.05$, $n = 9$). The shallowest nitracline depths (<70 m) and the highest nitrate diffusive fluxes (~ 2500 µmol N m^{-2} d^{-1}) were found in those stations under the influence of the equatorial upwelling (between 17°N and the Equator), while the deepest nitraclines (>100 m) were registered northwards of 20°N, coinciding with the lowest nitrate diffusive supply through the base of the euphotic layer. Therefore, both variables can be considered as proxies of the enhanced nitrate supply to the euphotic layer in those regions under the influence of the equatorial upwelling (Malone et al., 1993; Oschlies and Garcon, 1998). The magnitude of nitrate diffusive fluxes and the latitudinal pattern shown by this feature were also very similar to those reported by previous studies conducted in the central Atlantic Ocean (Planas et al., 1999) and by a recent analysis carried out for a similar latitudinal transect in 2008 (Mouriño-Carballido et al., 2011).

3.2. Total phytoplankton biomass, production and growth rates

The concentration of surface phytoplankton carbon biomass (Phyto-C) showed a marked increase in the equatorial upwelling region, where values >20 mg C m^{-3} were measured (Fig. 3c). Outside this region, Phyto-C took values around 10 mg C m^{-3}. A significant correlation between total Phyto-C and total chl a was found ($r = 0.87$, $p < 0.01$, $n = 10$). Surface total primary production varied from 0.5 ± 0.07 ($\pm$ sd) mg C m^{-3} d^{-1} to 6 ± 0.9 ($\pm$ sd) mg m^{-3} d^{-1} and total turnover rates ranged between 0.05 ± 0.007 ($\pm$ sd) d^{-1} and 0.2 ± 0.03 ($\pm$ sd) d^{-1}. In general, both variables showed a similar latitudinal pattern, with markedly higher values in the region affected by the equatorial upwelling (between 17°N and the Equator). Phytoplankton turnover rates increased to values of up to 0.2 d^{-1} in the region most affected by the upwelling, whereas values below 0.08 d^{-1} were estimated for the stations near both ends of the transect. In addition, a significant correlation between surface total primary production and euphotic layer-integrated total carbon fixation rates was also found ($r = 0.80$, $p < 0.01$, $n = 10$; euphotic layer-integrated primary production data were obtained from Moreno-Ostos et al., 2011).

3.3. Size-fractionated carbon biomass and production

Surface phytoplankton biomass was dominated by the <2 µm size fraction (picophytoplankton), with values between 4 and 20 mg C m^{-3} (Fig. 4a) and a relative contribution of $>40\%$ to total carbon biomass in most stations (Fig. 4c). Phytoplankton biomass of the 2–5 and 5–20 µm size fractions (small and large nanophytoplankton respectively) were much lower (0.3–3.2 mg C m^{-3}) with a relative contribution not higher than ca. 20% to total carbon biomass along the transect. In several stations between ca. 11°N and the Equator (latitudes affected by the equatorial upwelling), the carbon biomass represented by the size fraction >20 µm (microphytoplankton) was also relatively high with values varying between 11 and 17 µm C m^{-3}. This size class, with a relative contribution to total carbon biomass of ca. $>40\%$ in this region, displaced the picophytoplankton in their dominance of the phytoplankton biomass. This increase in the biomass of the microphytoplankton in this region was mainly due to the enhanced abundance of the filamentous cyanobacteria *Trichodesmium* spp. (Fernández et al., 2010), although the increase of the abundance of other diatom chain-former species was also observed (data not shown).

A higher degree of latitudinal variability was found in the contribution of the different size classes to carbon fixation rates (Fig. 4d). Although picophytoplankton showed, on average, the largest contribution to total production, the partitioning of carbon fixation among size classes (Fig. 4d) was more equitable than that of biomass (coefficient of variation between size classes for the relative contribution to total carbon fixation rate was always lower than that for the relative contribution to Phyto-C along the latitudinal transect, data not shown). All the size fractions showed a marked dome-like latitudinal pattern with higher production in the upwelling region (between 17°N and the Equator), although the degree of response to the environmental forcing associated with this hydrodynamic feature varied depending on the size class (Fig. 4b). While small nano- and large nano-phytoplankton primary production rates were between 0.1 ± 0.003–0.6 ± 0.05 ($\pm$ sd) mg C m^{-3} d^{-1} and 0.2 ± 0.02–0.7 ± 0.06 ($\pm$ sd) mg C m^{-3} d^{-1} respectively, pico- and micro-phytoplankton carbon fixation rates varied by ca. 16-fold and an opposite pattern in their relative contribution to total primary production was observed in the region of the equatorial upwelling (Fig. 4d).

The turnover rates of the pico- and small nano-phytoplankton typically ranged between 0.02 ± 0.002 ($\pm$ sd) and 0.3 ± 0.03 ($\pm$ sd) d^{-1}, and showed an increase (ca. 12- and 6-fold, respectively) in several stations affected by the upwelling (between 10°N and the Equator) (Fig. 5a and b). In general, the turnover rates of the large nanophytoplankton were higher, taking values in the range of 0.07 ± 0.01 ($\pm$ sd)–0.6 ± 0.06 ($\pm$ sd) d^{-1}, without a clear dome-like latitudinal pattern and varied slightly among stations throughout the equatorial upwelling domain (Fig. 5c). Finally, a higher latitudinal variability without a clear dome-like pattern was shown by microphytoplankton turnover rates,
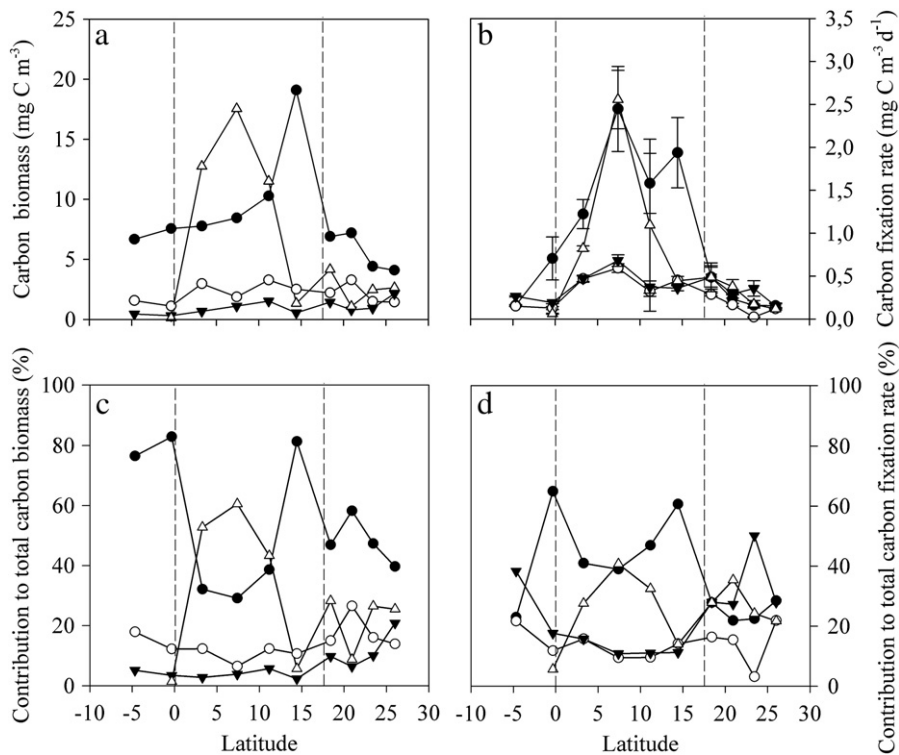
Fig. 4. Latitudinal variability of a) carbon biomass, b) carbon fixation rate, c) relative contribution (%) to total carbon biomass, d) relative contribution (%) to total carbon fixation rate of picophytoplankton (0.2–2 μm in ESD; black circles), small nanophytoplankton (2–5 μm in ESD; white circles), large nanophytoplankton (5–20 μm in ESD; black triangles) and microphytoplankton (>20 μm in ESD; white triangles). Error bars indicate 1 SD. Between vertical dashed lines are pointed out those stations under the influence of the equatorial upwelling. Latitude values as in Fig. 2.
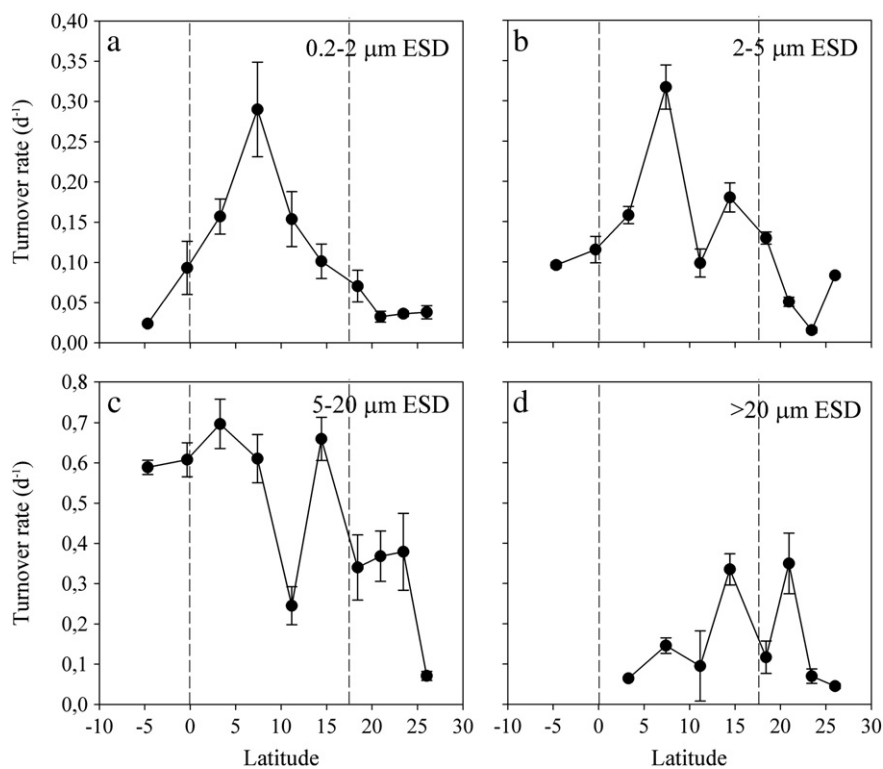

Fig. 5. Latitudinal variability of turnover rate of a) picophytoplankton (0.2–2 μm in ESD), b) small nanophytoplankton (2–5 μm in ESD), c) large nanophytoplankton (5–20 μm in ESD) and d) microphytoplankton (>20 μm in ESD). Error bars indicate 1 SD. Those stations under the influence of the equatorial upwelling are pointed out between vertical dashed lines. Latitude values as in Fig. 2.

whose values ranged between 0.04 ± 0.006 ($\pm$sd) and 0.35 ± 0.07 ($\pm$sd) d^{-1} along the transect (Fig. 5d).

The carbon fixation rate to chlorophyll a (chl a) concentration ratio of all size classes increased in the region most affected by the upwelling (Fig. 6). Throughout the transect, lower values were consistently found in the pico- and small nano-phytoplankton (range 1.4 ± 0.09 ($\pm$sd) to 14.5 ± 2.9 ($\pm$sd) mg C mg chl a^{-1} d^{-1}) than in the larger size classes (range from 3 ± 0.3 ($\pm$sd) to 35.5 ± 9.6 ($\pm$sd) mg C mg chl a^{-1} d^{-1}).

3.4. The influence of environmental forcing on size-fractionated carbon biomass, production and growth rates

In order to study the differential response of phytoplankton size fractions to changes in water column stability and nutrient input into the euphotic zone, we carried out a linear regression analysis between Brunt-Väisäla frequency (BV), nitracline depth, nitrate diffusive flux, Phyto-C, carbon fixation rate, turnover rate and the carbon fixation to chl a ratio (Tables 1 and 2). All the variables that did not meet the assumption of normality were log transformed before the statistical analysis. With the exception of microphytoplankton carbon biomass, which related with the water column stability ($r^2 = 0.58$, $p < 0.05$, $n = 9$), neither Brunt-Väisäla frequency nor nitracline depth showed any significant relationship with pico-, small nano- and large nano-phytoplankton biomass (Table 1). Primary production in all size fractions except large nanophytoplankton were related with BV ($r^2 = 0.46$–0.68, $p < 0.05$, $n = 10$), reflecting the association between higher stability and increased productivity in the upwelling region (Table 1). Conversely to that found for large nano- and micro-phytoplankton, the primary production, turnover rate and the carbon fixation to chl a ratio of pico- and small nano-phytoplankton showed an inverse significant relationship with nitracline depth (always $p < 0.05$), suggesting a stimulating effect of higher nutrient input in the euphotic layer on both absolute and biomass-specific productivity in

the smaller size classes (Tables 1 and 2). Although no significant relationships between nitrate diffusive flux and biotic variables were found, the similar latitudinal patterns shown by these variables in the central Atlantic Ocean (see Figs. 3B, 4 and 5) seem to suggest that there was an association between the increase in size-fractionated primary production, biomass and turnover rates found under the influence of the equatorial upwelling and the higher nitrate diffusive supply estimated for this region.

4. Discussion

The Atlantic equatorial upwelling constitutes a scenario of environmental forcing in which phytoplankton carbon biomass (Phyto-C) and primary production are stimulated (Marañón et al., 2000, 2001; Pérez et al., 2005b; Poulton et al., 2006). In our study, both Phyto-C values and primary production rates were similar to those previously reported for the same region (e.g. 6–47 mg C m^{-3} and 1.2–18 mg C m^{-3} d^{-1} respectively: Buck et al., 1996; Marañón et al., 2000), and the latitudinal pattern observed for both variables, characterised by higher values in those stations under the influence of the equatorial upwelling (between 17°N and the Equator) (Fig. 3c), coincided with previous studies in the Atlantic Ocean (Marañón et al., 2000; Morán et al., 2004; Pérez et al., 2005b). In addition, given the significant correlation found between surface and euphotic layer-integrated primary production ($p < 0.01$), we can consider that our surface measurements of total carbon fixation rate were representative of the primary production of the whole water column. Two new arising from our study should be highlighted. Firstly, in addition to the determination of phytoplankton primary production and chlorophyll a concentration, we also obtained direct biomass measurements, so phytoplankton turnover rates could be derived. Therefore, it was possible to elucidate whether the primary production enhancement observed under the upwelling influence was due only to the increased phytoplankton standing stocks, or if it was also the result of the
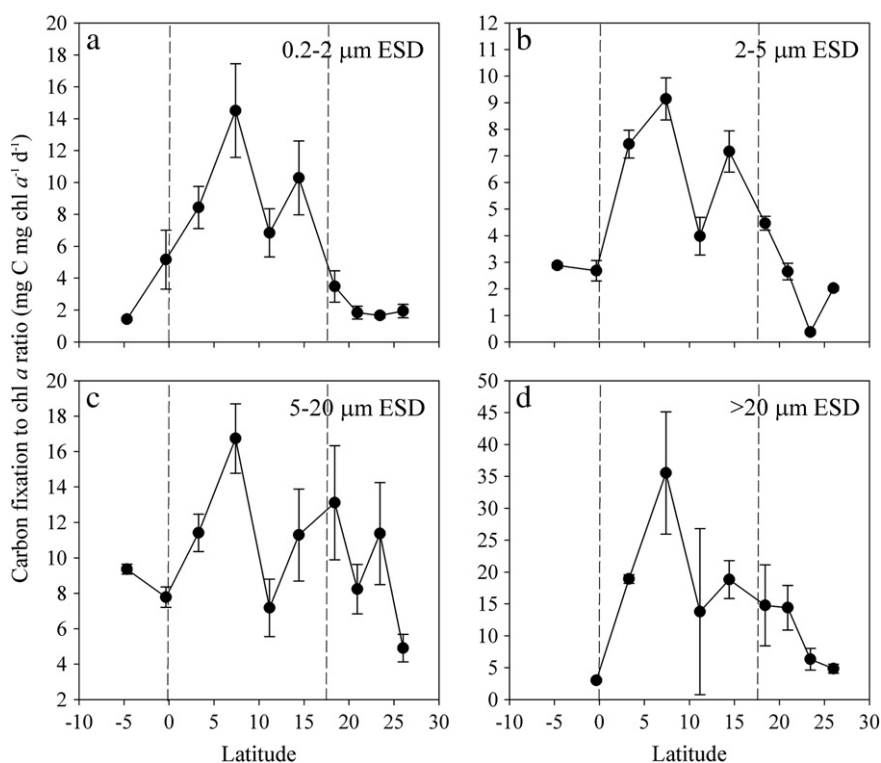
Fig. 6. Latitudinal variability of size-fractionated carbon fixation rate to chl a concentration ratio of a) picophytoplankton (0.2–2 μm in ESD), b) small nanophytoplankton (2–5 μm in ESD), c) large nanophytoplankton (5–20 μm in ESD) and d) microphytoplankton (>20 μm in ESD). Error bars indicate 1 SD. Those stations under the influence of the equatorial upwelling are pointed out between vertical dashed lines. Latitude values as in Fig. 2.

Table 1

Determination coefficients of the linear regression analysis conducted between phytoplankton biomass (mg C m^{-3}) and primary production (mg C m^{-3} d^{-1}) and water column stability, represented by Brunt-Väisäla frequency (BV freq.) (s^{-2}), nitrate diffusive flux (µmol N m^{-2} d^{-1}) and nitracline depth (m). Bt and Pt are total carbon biomass and total carbon fixation rate respectively. B0.2, B2, B5 and B20 refer to the carbon biomass of pico-, small nano-, large nano- and micro-phytoplankton. P0.2, P2, P5 and P20 refer to the carbon fixation rate of pico-, small nano-, large nano- and micro-phytoplankton. The linear regression P-values are between brackets. Bold data highlighted those relationships that are significant at 95%.

	Biomass					Primary production				
	Bt	B0.2	B2	B5	B20	Pt	P0.2	P2	P5	P20
BV freq.	**0.73**	0.21	0.18	−0.04	**0.58**	**0.63**	**0.68**	**0.68**	0.34	**0.46**
	(0.002)	(0.182)	(0.225)	(0.596)	**(0.017)**	**(0.006)**	**(0.003)**	**(0.004)**	(0.079)	**(0.046)**
Nitracline depth	**−0.51**	−0.44	−0.05	0.05	−0.22	**−0.50**	**−0.62**	**−0.53**	−0.16	−0.22
	(0.032)	(0.051)	(0.562)	(0.567)	(0.243)	**(0.047)**	**(0.012)**	**(0.026)**	(0.293)	(0.237)
Nitrate diffusive flux	0.30	0.35	0.19	0.02	0.04	0.14	0.21	0.30	0.17	0.21
	(0.124)	(0.095)	(0.243)	(0.755)	(0.624)	(0.313)	(0.219)	(0.134)	(0.265)	(0.256)

favourable effect of environmental forcing, mainly nutrient inputs, on phytoplankton physiology, translated into higher phytoplankton growth rates. Secondly, phytoplankton biomass, primary production and turnover rates were estimated in four different size classes, so we have been able to determine if there was a differential response among different phytoplankton groups to the environmental forcing associated with the equatorial upwelling. The results of this size-fractionated analysis conducted from surface samples can be extrapolated to the rest of the water column, as the geographical variability in phytoplankton size structure along latitudinal transects in the Atlantic is much higher than the variability observed in the vertical profiles (Marañón et al., 2001; Moreno-Ostos et al., 2011).

4.1. Changes in size-fractionated biomass and production in response to environmental forcing

Relatively few studies have previously analysed the partitioning of phytoplankton carbon biomass and carbon fixation rates among several size classes and over large spatial scales in the Atlantic Ocean (Buck et al., 1996; Marañón et al., 2001; Pérez et al., 2006; Poulton et al., 2006). It is commonly accepted that picophytoplankton biomass and production in the ocean keep relatively constant, independently of changes in the environment (Raimbault et al., 1988; Rodríguez et al., 1998; Thingstad and Sakshaug, 1990). However, our results confirm that not only microphytoplankton biomass and productivity respond to the environmental forcing associated with the equatorial upwelling, but also the other phytoplankton size classes identified, even the picophytoplankton, increased their carbon fixation rates in those stations under the influence of the upwelling. If we examine the latitudinal pattern of size-fractionated Phyto-C and carbon fixation rates (Fig. 4a and b) and also the relationships found between these variables and the Brunt-Väisäla frequency and nutrient supply (as reflected in the vertical diffusive flux of nitrate and also on the location of the nitracline depth) (Table 1, see P-values and determination coefficients), we can see that the response to the environmental forcing associated with the equatorial upwelling of all the size fractions was more intense in terms of primary production

than in carbon biomass. This result reflects the fact that phytoplankton standing stocks are also influenced by loss processes such as grazing and sedimentation rates (Kiørboe, 1993). As a consequence of this differential response in terms of biomass and production to the nutrient enrichment and the increased water-column stability, turnover rates were higher in those stations under the upwelling influence.

The effect of environmental forcing, reflected in changes in water column stability and nutrient supply, varied depending on the size class considered. While, with the exception of large nanophytoplankton, primary production of all phytoplankton size fractions showed a significant positive relationship with the water column stability, only pico- and small nano-phytoplankton carbon fixation rates respond significantly to the enhanced supply of nitrate into the euphotic layer (Table 1, see P-values and determination coefficients). Although this result contrasts with that previously reported by other authors (Landry et al., 1996; McAndrew et al., 2007; Poulton et al., 2006) and with the commonly accepted preference of smaller cells for the ammonium (Chisholm, 1992; Sunda and Hardison, 2010), it would confirm the observations by Glover et al. (2007) regarding the physiological response of picophytoplankton to nitrate perturbations. In their addition experiments conducted in the Sargasso Sea, these authors showed an enhancement of picophytoplankton photosynthesis in response to nanomolar nitrate supplements. Similarly, from the results derived from the JGOFS programme, Barber and Hiscock (2006) concluded that other phytoplankton taxa, in addition to diatoms, are able to respond by increasing their growth rates during the development of diatom-dominated blooms.

The fact that no significant relationship was found between large nano- and micro-phytoplankton production and the nitracline depth or nitrate diffusive flux may seem paradoxical, as it is well known that large phytoplankton grow mainly when resource availability increases (Chisholm, 1992; Kiørboe, 1993; Malone, 1980). In our survey, although other chain-forming species enhanced their abundance in those regions under the upwelling influence, the dominant species within microphytoplankton size class was the N$_2$-fixing cyanobacteria *Trichodesmium* spp., whose contribution to total Phyto-C was ~30%

Table 2

Determination coefficients of the linear regression analysis conducted between phytoplankton turnover rates, carbon fixation rate to chl *a* ratio and the water column structure, represented by Brunt-Väisäla frequency (BV freq.) (s^{-2}), nitrate diffusive flux (µmol N m^{-2} d^{-1}) and nitracline depth (m). Tt is the total turnover rate. T0.2, T02, T5 and T20 refer to the turnover rate of pico-, small nano-, large nano- and micro-phytoplankton and P/Chl0.2, P/Chl2, P/Chl5 and P/Chl20 refer to the carbon fixation rate to chl *a* ratio of pico-, small nano-, large nano- and micro-phytoplankton. The linear regression P-values are between brackets. Bold data highlighted those relationships that are significant at 95%.

	Turnover rate					Carbon fixation to chl *a* ratio			
	Tt	T0.2	T2	T5	T20	P/Chl0.2	P/Chl2	P/Chl5	P/Chl20
BV freq.	**0.57**	**0.69**	**0.47**	0.27	−0.01	**0.65**	**0.62**	0.14	0.37
	(0.011)	**(0.003)**	**(0.030)**	(0.124)	(0.846)	**(0.005)**	**(0.007)**	(0.295)	(0.083)
Nitracline depth	**−0.53**	**−0.45**	**−0.44**	−0.24	−0.03	**−0.54**	**−0.51**	−0.08	−0.21
	(0.026)	**(0.049)**	**(0.050)**	(0.184)	(0.724)	**(0.024)**	**(0.031)**	(0.464)	(0.251)
Nitrate diffusive flux	0.15	0.07	0.10	0.01	−0.01	0.13	0.23	0.09	0.09
	(0.307)	(0.496)	(0.417)	(0.846)	(0.879)	(0.339)	(0.187)	(0.444)	(0.488)

from 14°N to the Equator (data not shown). The presence of *Trichodesmium* spp. coincided with a higher rate of N_2 fixation between ca. 20°N and the Equator (Fernández et al., 2010). The dominance of microphytoplankton by a diazotroph species may explain the lack of relationship between the enhanced nitrate supply and the productivity of this phytoplankton size group in the region affected by the equatorial upwelling. Similarly, large nanophytoplankton was dominated mainly by dinoflagellates (data not shown), which present the competitive advantage of vertically migrating through the water column (Cullen and Horrigan, 1981). Thus, the effect of the equatorial enhanced nitrate supply on the carbon fixation rate of this size group may be masked by this ability to migrate vertically, which allows them to have access to the higher nitrate concentrations at the UML base.

As it has been found in previous studies carried out in the oligotrophic Atlantic Ocean (Buck et al., 1996; Marañón et al., 2001; Pérez et al., 2005b; Teira et al., 2005), along the whole latitudinal transect Phyto-C was dominated by picophytoplankton (relative contribution always >40%) and the contribution of the small and large nanophytoplankton never exceeded 20%. However, a marked shift in the relative contribution of pico- and micro-phytoplankton to total Phyto-C in those stations under the influence of the upwelling must be highlighted, as a decrease in the picophytoplankton biomass contribution of 40% coincided with an increase of ca. 50% in the contribution of microphytoplankton. Similarly, in these stations where the highest production was found, the highest contribution to total primary production was due to microphytoplankton and this peak coincided with a decrease of ca. 20% in the picophytoplankton contribution to total carbon fixation rate. However, as we discuss below (Section 4.2), our data suggest that the pico- and small nano-phytoplankton were the size classes that showed the strongest physiological response to the upwelling. Thus, the increased dominance of larger phytoplankton in the upwelling area may have been partly favoured by the retention effect of upward water motion (*e.g.* Rodríguez et al., 2001), as it is supported by the significant positive relationship found between microphytoplankton biomass and primary production and the water column stability (Table 1).

4.2. Influence of environmental forcing on growth rates

The knowledge of phytoplankton growth rates in combination with primary production rate and Phyto-C concentration is useful in order to elucidate whether the phytoplankton community is only limited in its standing stocks or also in its physiological state (Goldman et al., 1979). Moreover, by comparing the growth rates estimated with those expected for the temperatures registered it is possible to assess if phytoplankton are growing at their maximum theoretical rate (Eppley, 1972; Marañón, 2005). In our study, the turnover rates of the whole phytoplankton assemblage fall within the range of values estimated previously by several authors for the same oceanic regions (e. g. 0.05–0.2 d^{-1}: Goericke and Welschmeyer, 1998; Lessard and Murrel, 1998; Marañón 2005, among others). These values were clearly smaller than the maximum theoretical growth rates (~1.5 d^{-1}) estimated by Eppley (1972) for microalgae growing at the warm temperatures observed in tropical oceans. A nutrient limitation of phytoplankton growth has been suggested as an explanation for the suboptimal rates found (Marañón 2005). In addition, a significant inverse correlation between total growth rate and nitracline depth has been reported in basin-scale terms for the Atlantic Ocean (Marañón et al., 2000) and several experiments carried out in the tropical and subtropical Atlantic regions have shown compelling evidence of nutrient limitation of phytoplankton physiology and growth (Graziano et al., 1996; Martínez-García et al., 2010; Mills et al., 2004; Moore et al., 2008). In our case, the association, observed in the upwelling region (between 17°N and the Equator), between increased nitrate diffusive fluxes, shallower nitracline

depths and enhanced total phytoplankton turnover rates strongly suggests a response of phytoplankton growth to nitrate supply. This response was also evidenced by the significant relationship found between total turnover rates and nitracline depth (Table 2). Therefore, not only phytoplankton standing stocks but also their physiological states were limited by nitrate availability.

Most previous studies on phytoplankton growth rates in specific size classes have focused on the <2 μm size fraction (Hirose et al., 2008; Liu et al., 1997; Zubkov and Tarran, 2008; among others). To the best of our knowledge only Pérez et al. (2006) and Poulton et al. (2006) reported some growth rates estimations for all phytoplankton in the >2um size fraction, so our study is the first assessment of the variability in phytoplankton turnover rates of four different size classes over basin-wide scales. The estimated picophytoplankton turnover rates were within the range reported by previous studies for the same region (Pérez et al., 2006; Poulton et al., 2006) and both pico- and small nano-phytoplankton turnover rates were, in general, much lower than those estimated for large nano- and micro-phytoplankton. This observation contrasts with the higher growth rates expected for small-sized phytoplankton, if we consider their advantage over larger cells in nutrient-poor environments (Raven and Kübler, 2002). In addition, recent studies have reported that phytoplankton taxonomic groups with a larger average size such as diatoms sustain higher growth rates than other taxonomic groups that belong to the pico- and nano-phytoplankton size range, such as green algae or prymnesiophytes (Latasa et al., 2005). These results highlight the importance of determining the growth rates of different taxonomic and size categories, because a single, overall turnover rate for the whole community often masks the presence of contrasting growth dynamics in different algal groups. As a result, the relative importance of different groups in terms of carbon fluxes can vary considerably (Latasa et al., 2005). Thus, we can conclude that in our study the large nano- and the micro-phytoplankton contributed to primary production more than what could be expected on the basis of their biomass share. This feature has been reported previously for the oligotrophic oceans (Fernández et al., 2003; Malone et al., 1993; Tremblay and Legendre, 1994), and it has been commonly explained by the preferential removal of larger cells by sinking and grazing processes (Fernández et al., 2003; Tremblay and Legendre, 1994) or the higher damage cell of small phytoplankton in these oceanic regions (Agustí et al., 1998; Moreno-Ostos et al., 2011). In our case, the higher turnover rates estimated for large nano- and micro-phytoplankton, in addition to the higher carbon fixation rate to chl *a* ratios obtained, would add an additional explanation to this general pattern (Poulton et al., 2006; Teira et al., 2005).

The dome-like latitudinal pattern showed by pico- and small nano-phytoplankton turnover rates, with higher rates coinciding with shallower nitracline depths and higher nitrate diffusive fluxes, indicates that these small-celled photoautotrophs were the most responsive to the enhanced nitrate supply in the equatorial region. This result is supported by the significant relationships found between the turnover rates and carbon fixation rate to chl *a* ratios estimated for pico- and small nano-phytoplankton and the nitracline depth, which contrast with the lack of relationship for large nano- and micro-phytoplankton (Table 2). The fact that the smaller phytoplankton, rather than the larger cells, responded to the enhanced nitrate supply with an increase in their turnover rates and carbon fixation rate to chl *a* ratios must be interpreted taking into account the dynamics of the equatorial upwelling. Coastal upwelling and water mixing events occur episodically in pelagic ecosystems, and cause sudden and large increases in the available nutrient concentration. In this scenario, large-sized phytoplankton such as diatoms are strongly favoured by their high maximal uptake rates and nutrient storage capacities (Litchman et al., 2007; Sarthou et al., 2005; Thingstad et al., 2005; Verdy et al., 2009), resulting in their dominance of the phytoplankton community (Margalef, 1978; Smayda and Reynolds, 2001). In

contrast, the equatorial upwelling, although subject to temporal variability (Longhurst, 1993; Pérez et al., 2005a), represents a more steady hydrodynamic feature that results in modest and persistent increases in nutrient supply. In our study, although the nutrient supply rate into the euphotic layer was clearly enhanced in the upwelling region, nitrate concentration never exceeded 0.2 μmol L^{-1} in the upper mixed layer. Thus, the more marked growth response of small phytoplankton would be a result of the small magnitude of the nutrient input and its relatively continuous nature, which provide a competitive advantage to small cells adapted to oligotrophic conditions (Cermeño et al., 2011; Verdy et al., 2009). In addition to the competitive disadvantage of larger cells in this kind of hydrodynamic feature, the lack of response of large nano- and micro-phytoplankton to the enhanced nitrate supply in the equatorial upwelling would be due to the dominant taxonomic composition of these size groups. Whereas the N_2 fixation carried out by *Trichodesmium* spp. would be providing of an additional nutrient supply to the microphytoplankton, the ability of dinoflagellates to migrate vertically would allow them not to depend exclusively on nitrate supply from below the UML.

In summary, the observed increase of both phytoplankton primary production and turnover rates to the enhanced nitrate supply in the equatorial upwelling suggests that phytoplankton physiology was nutrient limited in the oligotrophic central Atlantic Ocean. In addition, our results highlight the importance of conducting simultaneously size-fractionated analysis of phytoplankton standing stocks and metabolism, when the aim is to obtain a more comprehensive picture of the dynamics of phytoplankton communities and their role in the functioning of pelagic ecosystems. The higher responsiveness found of small-sized phytoplankton fractions to the nutrient enrichment also stress the relevance of considering not only the magnitude of nutrient supply, but also the rate of this supply when analysing the physiological response of phytoplankton size groups. Given the contrasting role of large and small phytoplankton size classes in terms of trophic interactions and potential carbon export in pelagic ecosystems, this kind of studies will be complementary to those analyses focussed on the response of the phytoplankton community as a whole.

Acknowledgements

References

Agustí, S., Satta, M.P., Mura, M.P., Benavent, E., 1998. Dissolved sterase activity as a tracer of phytoplankton lysis: evidence of high phytoplankton lysis rates in the southwestern Mediterranean. Limnol. Oceanogr. 43, 1836–1849.

Azam, F., Fenchel, T., Field, J.G., Gray, J.S., Seyer-Reil, M.A., Thingstad, F., 1983. The ecological role of water-column microbes in the sea. Mar. Ecol. Prog. Ser. 10, 257–263.

Barber, R.T., Hiscock, M.R., 2006. A rising tide lifts all phytoplankton: growth response of other phytoplankton taxa in diatom-dominated blooms. Global Biogeochem. Cycles 20, GB4S03. doi:10.1029/2006GB002726.

Bray, N.A., Fofonoff, N.P., 1981. Available potential energy for MODE eddies. J. Phys. Oceanogr. 10, 30–46.

Buck, K.R., Chávez, F.P., Campbell, L., 1996. Basin-wide distributions of living carbon components and the inverted trophic pyramid of the central gyre of the North Atlantic Ocean, summer 1993. Aquat. Microb. Ecol. 10, 283–298.

Calvo-Díaz, A., Morán, X.A., 2006. Seasonal dynamics of picoplankton in shelf waters of the southern Bay of Biscay. Aquat. Microb. Ecol. 42, 159–174.

Cermeño, P., Marañón, E., Rodríguez, J., Fernández, E., 2005a. Large-sized phytoplankton sustain higher carbon-specific photosynthesis than smaller cells in a coastal eutrophic ecosystem. Mar. Ecol. Prog. Ser. 297, 51–60.

Cermeño, P., Lee, J.B., Wyman, J., Schofield, O., Falkowski, P.G., 2011. Competitive dynamics in two species of marine phytoplankton under non-equilibrium conditions. Mar. Ecol. Prog. Ser. 429, 19–28.

Chisholm, S.W., 1992. Phytoplankton size. In: Falkowski, P.G., Woodhead, A.D. (Eds.), Primary Productivity and Biogeochemical Cycles in the Sea. Plenum Press, New York, pp. 213–236.

Cullen, J.J., Horrigan, S.G., 1981. Effects of nitrate on the diurnal vertical migration, carbon to nitrogen ratio, and the photosynthetic capacity of the dinoflagellate *Gymnodinium splendens*. Mar. Biol. 62, 81–89.

Cushing, D.H., 1989. A difference in structure between ecosystems in strongly stratified waters and in those that are only weaked stratified. J. Plankton Res. 11, 1–13.

Eppley, R.W., 1972. Temperature and phytoplankton growth in the sea. Fish. Bull. 70, 1063–1085.

Fernández, E., Marañón, E., Morán, X.A.G., Serret, P., 2003. Potential causes for the unequal contribution of picophytoplankton to total biomass and productivity in oligotrophic waters. Mar. Ecol. Prog. Ser. 254, 101–109.

Fernández, A., Mouriño-Carballido, B., Bode, A., Varela, M., Marañón, E., 2010. Latitudinal distribution of *Trichodesmium* spp. and N_2 fixation in the Atlantic Ocean. Biogeosciences 7, 2198–2225.

Geider, R.J., 1992. Respiration: taxation without representation? In: Falkowski, P.G., Woodhead, A.D. (Eds.), Primary Productivity and Biogeochemical Cycles in the Sea. Plenum Press, New York, pp. 333–360.

Glover, H.E., Garside, C., Trees, C.C., 2007. Physiological responses of Sargasso Sea picoplankton to nanomolar nitrate perturbations. J. Plankton Res. 29, 263–274.

Goericke, R., Welschmeyer, N.A., 1998. Response of Sargasso Sea phytoplankton biomass, growth rates and primary production to seasonally varying physical forcing. J. Plankton Res. 20, 2223–2249.

Goldman, J.C., 1988. Spatial and temporal discontinuities of biological processes in pelagic surface waters. In: Rothschild, B.J. (Ed.), Towards a Theory on Biological–Physical Interactions in the World Ocean. Kluwer Academic Publishers, Netherlands, pp. 273–296.

Goldman, J.C., McCarthy, J.J., Peavey, D.G., 1979. Growth rate influence on the chemical composition of phytoplankton in oceanic waters. Nature 279, 210–215.

Graziano, L.M., Geider, R.J., Li, W.K.W., Olaizola, M., 1996. Nitrogen limitation of North Atlantic phytoplankton: analysis of physiological condition in nutrient enrichment experiments. Aquat. Microb. Ecol. 11, 53–64.

Han, M.-S., Furuya, K., 2000. Size and species-specific primary productivity and community structure of phytoplankton in Tokyo Bay. J. Plankton Res. 22, 1221–1235.

Herbland, A., Voituriez, B., 1979. Hydrological structure analysis for estimating the primary production in the tropical Atlantic Ocean. J. Mar. Res. 37, 87–101.

Hirose, M., Katano, T., Nakano, S.I., 2008. Growth and grazing mortality rates of Prochlorococcus, Synechococcus and eukaryotic picophytoplankton in a bay of the Uwa Sea, Japan. J. Plankton Res. 30, 241–250.

Jochem, F., Zeitzschel, B., 1989. Productivity regime and phytoplankton size structure in the tropical and subtropical North Atlantic in spring. Deep Sea Res. II Top. Stud. Oceanogr. 40, 495–519.

Joint, I.R., Pomroy, A.J., 1986. Photosynthetic characteristics of nanoplankton and picoplankton from the surface mixed layer. Mar. Biol. 92, 465–474.

Kiørboe, T., 1993. Turbulence, phytoplankton cell size, and the structure of pelagic food webs. Adv. Mar. Biol. 29, 1–72.

Kirchman, D.L., 2002. Calculating microbial growth rates from data on production and standing stocks. Mar. Ecol. Prog. Ser. 233, 303–306.

Landry, M.R., Kirshtein, J., Constantinou, J., 1996. Abundances and distributions of picoplankton populations in the central equatorial Pacific from 12°N to 12°S, 140°W. Deep Sea Res. II Top. Stud. Oceanogr. 43, 871–890.

Large, W.G., Pond, S., 1981. Open ocean momentum flux measurements in moderate strong winds. J. Phys. Oceanogr. 11, 324–336.

Latasa, M., Morán, X.A.G., Scharek, R., Estrada, M., 2005. Estimating the carbon flux through main phytoplankton groups in the northwestern Mediterranean. Limnol. Oceanogr. 50, 1447–1458.

Legendre, L., Rassoulzadegan, F., 1996. Food-web mediated export of biogenic carbon in oceans: hydrodynamic control. Mar. Ecol. Prog. Ser. 145, 179–193.

Lessard, E.J., Murrel, M.C., 1998. Microzooplankton herbivory and phytoplankton growth in the northwestern Sargasso Sea. Aquat. Microb. Ecol. 16, 173–188.

Li, W.K.W., Harrison, W.G., 2001. Chlorophyll, bacteria and picophytoplankton in ecological provinces of the North Atlantic. Deep Sea Res. I. Oceanogr. Res. Pap. 48, 2271–2293.

Li, W.K.W., Harrison, W.G., Head, E.J.H., 2006. Coherent assembly of phytoplankton communities in diverse temperate ocean ecosystems. Proc. R. Soc. Lond. B Biol. Sci. 273, 1953–1960.

Litchman, E., Klausmeier, C.A., Schofield, O.M., Falkowski, P.G., 2007. The role of functional traits and trade-offs in structuring phytoplankton communities: scaling from cellular to ecosystem level. Ecol. Lett. 10, 1170–1181.

Liu, H., Nolla, H.A., Campbell, L., 1997. Prochlorococcus growth rate and contribution to primary production in the equatorial and subtropical North Pacific Ocean. Aquat. Microb. Ecol. 12, 39–47.

Longhurst, A., 1993. Seasonal cooling and blooming in the tropical oceans. Deep Sea Res. I Oceanogr. Res. Pap. 40, 2145–2165.

Longhurst, A., 1995. Seasonal cycles of pelagic production and consumption. Prog. Oceanogr. 36, 77–167.

Lund, J.W.G., Kipling, C., Le Cren, E.D., 1958. The inverted microscope method of estimating algal numbers and the statistical basis of estimations by counting. Hydrobiologia 11, 143–170.

Malone, T.C., 1980. Algal size. In: Morris, I. (Ed.), The Physiological Ecology of Phytoplankton. Blackwell Scientific Publications, London, pp. 433–463.

Malone, T.C., Pike, S.E., Conley, D.J., 1993. Transient variations in phytoplankton productivity at the JGOFS Bermuda time series station. Deep Sea Res. I Oceanogr. Res. Pap. 40, 903–924.

Marañón, E., 2005. Phytoplankton growth rates in the Atlantic subtropical gyres. Limnol. Oceanogr. 50, 299–310.

Marañón, E., 2009. Phytoplankton size structure. In: Steele, J.H., Turekian, K.K., Thorpe, S.A. (Eds.), Encyclopedia of Ocean Science. Academic Press, Oxford.

Marañón, E., Holligan, P.M., Varela, M., Mouriño, B., Bale, A.J., 2000. Basin-scale variability of phytoplankton biomass, production and growth in the Atlantic Ocean. Deep Sea Res. I Oceanogr. Res. Pap. 47, 825–857.

Marañón, E., Holligan, P.M., Barciela, R., González, N., Mouriño, B., Pazó, M.J., Varela, M., 2001. Patterns of phytoplankton size structure and productivity in contrasting open-ocean environments. Mar. Ecol. Prog. Ser. 216, 43–56.

Margalef, R., 1978. Life-forms of phytoplankton as survival alternatives in an unstable environment. Oceanolog. Acta 1, 493–509.

Marie, D., Partensky, F., Vaulot, D., 1999. Enumeration of phytoplankton, bacteria, and viruses in marine samples. In: Robinson, J.P. (Ed.), Current Protocols in Cytometry. John Wiley and Sons, New York, pp. 11.11.1–11.11.15.

Martínez-García, S., Fernández, E., Calvo-Díaz, A., Marañón, E., Morán, X.A.G., Teira, E., 2010. Response of heterotrophic and autotrophic microbial plankton to inorganic and organic inputs along a latitudinal transect in the Atlantic Ocean. Biogeosciences 7, 1701–1713.

McAndrew, P.M., Björkman, K.M., Church, M.J., Morris, P.J., Jachowski, N., Williams, P.J. leB., Karl, D.M., 2007. Metabolic response of oligotrophic plankton communities to deep water nutrient enrichment. Mar. Ecol. Prog. Ser. 332, 63–75.

Mills, M.M., Ridame, C., Davey, M., La Roche, J., Geider, R.J., 2004. Iron and phosphorous co-limit nitrogen fixation in the eastern tropical North Atlantic. Nature 429, 292–294.

Monger, B., McClain, C., Murtugudde, R., 1997. Seasonal phytoplankton dynamics in the eastern tropical Atlantic. J. Geophys. Res. 102, 12389–12411.

Montagnes, D.J.S., Berges, J.A., 1994. Estimating carbon, nitrogen, protein, and chlorophyll *a* from volume in marine phytoplankton. Limnol. Oceanogr. 39, 1044–1060.

Moore, C.M., Mills, M.M., Langlois, R., Milne, A., Achterberg, E.P., LaRoche, J., Geider, R.J., 2008. Relative influence of nitrogen and phosphorous availability on phytoplankton physiology and productivity in the oligotrophic sub-tropical North Atlantic Ocean. Limnol. Oceanogr. 53, 291–305.

Morán, X.A.G., Fernández, E., Pérez, V., 2004. Size-fractionad primary production, bacterial production and net community production in subtropical and tropical domains of the oligotrophic NE Atlantic in autumn. Mar. Ecol. Prog. Ser. 274, 17–29.

Moreno-Ostos, E., Fernández, A., Huete-Ortega, M., Mouriño-Carballido, B., Calvo-Díaz, A., Morán, X.A.G., Marañón, E., 2011. Size-fractionated phytoplankton biomass and production in the tropical Atlantic Ocean: dynamics of picophytoplankton. Sci. Mar. 75, 379–389.

Mouriño-Carballido, B., Graña, R., Fernández, A., Bode, A., Varela, M., Domínguez, J.F., Escánez, J., de Armnas, D., Marañón, E., 2011. Importance of N₂ fixation vs. nitrate eddy diffusion along a latitudinal transect in the Atlantic Ocean. Limnol. Oceanogr. 56, 999–1007.

Olenina, I., Hajdu, S., Edler, L., Andersson, A., Wasmund, N., Busch, S., Göbel, J., Gromisz, S., Huseby, S., Huttunen, M., Jaanus, A., Kokkonen, P., Ledaine, I., Niemkiewicz, E., 2006. Biovolumes and size-classes of phytoplankton in the Baltic Sea. HELCOM Baltic Sea Environment Proceedings, 106.

Osborn, T.R., 1980. Estimates of the local rate of vertical diffusion from dissipation measurements. J. Phys. Oceanogr. 10, 83–89.

Oschlies, A., Garcon, V., 1998. Eddy-induced enhancement of primary production in a model of the North Atlantic Ocean. Nature 394, 266–269.

Parsons, T.R., Takahashi, M., 1973. Environmental control of phytoplankton cell size. Limnol. Oceanogr. 28, 511–515.

Partensky, F., Blanchot, B., Lantoine, F., Neveux, J., Marie, D., 1996. Vertical structure of picophytoplankton at different trophic sites of the tropical northeastern Atlantic Ocean. Deep Sea Res. I Oceanogr. Res. Pap. 43, 1191–1213.

Pérez, V., Fernández, E., Marañón, E., Serret, P., García-Soto, C., 2005a. Seasonal and interannual variability of chlorophyll *a* and primary production in the Equatorial Atlantic: 'in situ' and remote sensing observations. J. Plankton Res. 27, 189–197.

Pérez, V., Fernández, E., Marañón, E., Serret, P., Varela, R., Bode, A., Varela, M., Varela, M.M., Morán, X.A.G., Woodward, E.M.S., Kitidis, V., García-Soto, C., 2005b. Latitudinal distribution of microbial plankton abundance, production, and respiration in the Equatorial Atlantic in autumn 2000. Deep Sea Res. I Oceanogr. Res. Pap. 52, 861–880.

Pérez, V., Fernández, E., Marañón, E., Morán, X.A.G., Zubkov, M.V., 2006. Vertical distribution of phytoplankton biomass, production and growth rate in the Atlantic subtropical gyres. Deep Sea Res. I Oceanogr. Res. Pap. 53, 1616–1634.

Planas, D., Agustí, S., Duarte, C.M., Granata, T.C., Merino, M., 1999. Limnol. Oceanogr. 44, 116–126.

Poulton, A.J., Holligan, P.M., Hickman, A., Kim, Y.-N., Adey, T.R., Stichcombe, M.C., Holeton, C., Root, S., Woodward, E.M.S., 2006. Phytoplankton carbon fixation, chlorophyll-biomass and diagnostic pigments in the Atlantic Ocean. Deep Sea Res. II Top. Stud. Oceanogr. 53, 1593–1610.

Raimbault, P., Rodier, M., Taupier-Letage, I., 1988. Size fraction of phytoplankton in the Ligurian Sea and the Algerian Basin (Mediterranean Sea): size distribution versus total concentration. Mar. Microb. Food Webs 3, 1–7.

Raimbault, P., Slawyk, G., Coste, B., Fry, J., 1990. Feasibility of using an automated colorimetric procedure for the determination of seawater nitrate in the 0 to 100 nM range: examples from field and culture. Mar. Biol. 104, 347–351.

Raven, J.A., Kübler, J.E., 2002. New light on the scaling of metabolic rate with the size of algae. J. Phycol. 38, 11–16.

Rodríguez, J., Blanco, J.M., Jimenez, F., Echevarría, F., Gil, J., Rodriguez, V., Ruiz, J., Bautista, B., Guerrero, F., 1998. Patterns in the size structure of the phytoplankton community in the deep fluorescence maximum of the Alboran Sea (southwestern Mediterranean). Deep Sea Res. I Oceanogr. Res. Pap. 45, 1577–1593.

Rodríguez, J., Tintoré, J., Allen, J.T., Blanco, J.M., Gomis, D., Reul, A., Ruíz, J., Rodríguez, V., Echevarría, F., Jiménez-Gómez, F., 2001. Mesoscale vertical motion and the size structure of phytoplankton in the ocean. Nature 410, 360–363.

Sarthou, G., Timmermans, K.R., Blain, S., Tréguer, P., 2005. Growth physiology and fate of diatoms in the ocean: a review. J. Sea Res. 53, 25–42.

Sieburth, J. McN, 1979. Sea Microbes. Oxford University Press, New York.

Smayda, T.J., Reynolds, C.S., 2001. Community assembly in marine phytoplankton: application of recent models to harmful dinoflagellate blooms. J. Plankton Res. 23, 447–461.

Sunda, W.G., Hardison, D.R., 2010. Evolutionary tradeoffs among nutrient acquisition, cell size, and grazing defense in marine phytoplankton ecosystem stability. Mar. Ecol. Prog. Ser. 401, 63–76.

Tamigneaux, E., Legendre, L., Klein, B., Mingelbier, M., 1999. Seasonal dynamics and potential fate of size-fractionated phytoplankton in a temperate nearshore environment (Western Gulf of St. Lawrence, Canada). Est. Coast. Shelf. Sci. 48, 253–269.

Tarran, G., Heywood, J.L., Zubkov, M.V., 2006. Latitudinal changes in the standing stocks of nano- and picoeukaryotic phytoplankton in the Atlantic Ocean. Deep Sea Res. II Top. Stud. Oceanogr. 53, 1516–1529.

Teira, E., Mouriño, B., Marañón, E., Pérez, V., Pazó, M.J., Serret, P., Fernández, E., 2005. Variability of chlorophyll and primary production in the Eastern North Atlantic subtropical gyre: potential factors affecting phytoplankton activity. Deep Sea Res I Oceanogr. Res. Pap. 52, 569–588.

Terray, E.A., Donelan, M.A., Agrawal, Y.C., Drennan, W.M., Kahma, K.K., Williams III, A.J., Hwang, P.A., Kitaigorodskii, S.A., 1996. Estimates of kinetic energy dissipation under breaking waves. J. Phys. Oceanogr. 26, 792–807.

Thingstad, T.F., Sakshaug, E., 1990. Control of phytoplankton growth in nutrient recycling ecosystems. Theory and terminology. Mar. Ecol. Prog. Ser. 63, 261–272.

Thingstad, T.F., Øvreås, L., Egge, J.K., Løvdal, T., Heldal, M., 2005. Use of non-limiting substrates to increase size; a generic strategy to simultaneously optimize uptake and minimize predation in pelagic osmotrophs? Ecol. Lett. 8, 675–682.

Tomczak, M., Godfrey, J.S., 1994. Regional Oceanography: An Introduction. Pergamon, New York.

Tremblay, J.E., Legendre, L., 1994. A model for the size-fractionated biomass and production of marine phytoplankton. Limnol. Oceanogr. 39, 2004–2014.

Verdy, A., Follows, M., Flierl, G., 2009. Optimal phytoplankton cell size in an allometric model. Mar. Ecol. Prog. Ser. 379, 1–12.

Verity, P.G., Robertson, C.Y., Tronzo, C.R., Andrews, M.G., Nelson, J.R., Sieracki, M.E., 1992. Relationships between cell volume and the carbon and nitrogen content of marine photosynthetic nanoplankton. Limnol. Oceanogr. 37, 1434–1446.

Worden, A.Z., Nolan, J.K., Palenik, B., 2004. Assessing the dynamics and ecology of marine picophytoplankton: the importance of the eukaryotic component. Limnol. Oceanogr. 49, 168–179.

Zubkov, M.V., Tarran, G.A., 2008. High bacterivory by the smallest phytoplankton in the North Atlantic. Nature 455, 224–226.

Zubkov, M.V., Sleigh, M.A., Tarran, G.A., Burkill, P.H., Leakey, R.J.G., 1998. Picoplanktonic community structure on an Atlantic transect from 50°N to 50°S. Deep Sea Res. I Oceanogr. Res. Pap. 45, 1339–1355.